TU-866, KEK-TH-1355
April 12, 2010

Violation of Casimir Scaling for Static QCD Potential at Three-loop Order

C. Anzai[a], Y. Kiyo[b] and Y. Sumino[a]

[a] *Department of Physics, Tohoku University*
Sendai, 980-8578 Japan
[b] *Theory Center KEK, Tsukuba*
Ibaraki 305-0801, Japan

Abstract

We compute the full $\mathcal{O}(\alpha_s^4)$ and $\mathcal{O}(\alpha_s^4 \log \alpha_s)$ corrections to the potential $V_R(r)$ between the static color sources, where $V_R(r)$ is defined from the Wilson loop in a general representation R of a general gauge group G. We find a violation of the Casimir scaling of the potential, for the first time, at $\mathcal{O}(\alpha_s^4)$. The effect of the Casimir scaling violation is predicted to reduce the tangent of $V_R(r)/C_R$ proportionally to specific color factors dependent on R. We study the sizes of the Casimir scaling violation for various R's in the case $G = SU(3)$. We find that they are well within the present bounds from lattice calculations, in the distance region where both perturbative and lattice computations of $V_R(r)$ are valid. We also discuss how to test the Casimir scaling violating effect.

PACS numbers: 12.38.Aw, 12.38.Bx, 14.40.Pq

1 Introduction

The nature of the strong force is still a subject studied widely today. In particular, the static QCD potential has been studied extensively for the purpose of elucidating the nature of the interaction between static color sources. The static potential is a generalization of the Coulomb potential in QED to the case of QCD. Generally, the static potential at short-distances can be computed accurately by perturbative QCD. On the other hand, the static potential at long-distances should be determined by non-perturbative methods, such as lattice simulations or computations based on various models.

Since some time, lattice computations have shown that the static QCD potentials between the color sources in various color representations (in the color-singlet channel) exhibit a property known as "Casimir scaling," within accuracies better than 5%, and in the distance range 0.1 fm $\lesssim r \lesssim$ 1 fm [1, 2].[1] Casimir scaling is a property of the static potential $V_R(r)$ between the color sources in the representation R, that the dependence of $V_R(r)$ on R is given only by an overall factor C_R, the eigenvalue of the quadratic Casimir operator for the representation R. It turned out [5] that the Casimir scaling property of the static potential is a powerful discriminant of various models and approaches, which attempt to explain the nature of the QCD vacuum and color confinement. So far, however, a reasoning of Casimir scaling from the first principle has been missing.

Computations of the static potentials in perturbative QCD have steadily made progress over decades. In particular, the discovery of the cancellation of the renormalons in the total energy of a static quark-antiquark pair led to a drastic improvement in the accuracy of the perturbative prediction of the static potential between the fundamental charges [6]. At the same time, the distance range, in which lattice computations and perturbative prediction agree with each other, extended to a significantly wider range [7, 8, 9]. By renormalization-group improvement of the perturbative prediction (after subtracting the renormalon), this overlap range extended to 0.05 fm $\lesssim r \lesssim$ 0.4 fm [10]. It was shown that non-perturbative contributions to the static potential in this overlap region are much smaller than previous estimates, once the renormalon cancellation is incorporated in the perturbative computations. The linear potential (whose size is determined from the long-distance behavior of the potential) is excluded as a non-perturbative contribution in this distance region. Furthermore, it was shown analytically that the perturbative static potential approaches a "Coulomb+linear" form in the above distance range due to the higher-order terms of the perturbative expansion, on the basis of a renormalon-dominance picture [11].

Recently two groups (including our group) have independently completed computations of the 3-loop corrections to the static potential between two fundamental color representations [12, 13]. Compiling our present knowledge, the perturbative expansion of the static potential between the fundamental charges is known up to $\mathcal{O}(\alpha_s^4)$ and also all the logarithmic terms at $\mathcal{O}(\alpha_s^5)$ [14, 15] in this expansion are known. Comparatively, the perturbative expansion of the static potential between the color sources in a general

[1] See [3, 4] for simulation studies on the Casimir scaling property for gauge groups other than $SU(3)$.

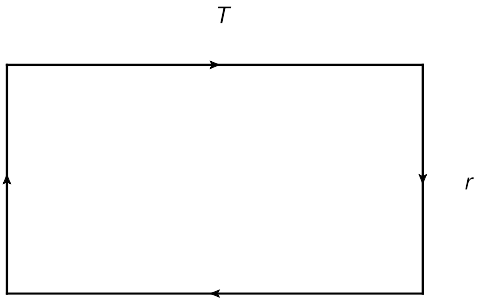

Figure 1: Contour C for the Wilson loop in $W_R[C]$.

color representation has been known only up to $\mathcal{O}(\alpha_s^3)$ [16]. The Casimir scaling is known to hold for the perturbative potential at least up to this order.

In this paper we compute the full $\mathcal{O}(\alpha_s^4)$ and $\mathcal{O}(\alpha_s^4 \log \alpha_s)$ corrections to the static potential between the color sources in a general color representation, for a general gauge group, by generalizing the computation for the potential for the fundamental representation. The $\mathcal{O}(\alpha_s^4)$ correction originates from the purely perturbative 3-loop correction, while the $\mathcal{O}(\alpha_s^4 \log \alpha_s)$ correction originates from the ultra-soft correction. We find that the Casimir scaling is violated, for the first time, at $\mathcal{O}(\alpha_s^4)$. In view of the consistency of the perturbative and lattice predictions for the fundamental potential, it is interesting to test consistency of the two predictions regarding the Casimir scaling. In particular, it is crucial whether the effects of the violation of the Casimir scaling by perturbative QCD exceed the current bounds from lattice computations. We examine the effects for various color representations within perturbative QCD and compare them with the lattice results. We also discuss how to test the perturbative prediction for the violation of the Casimir scaling.

In Sec. 2, after fixing our notations and conventions, we present our result for the $\mathcal{O}(\alpha_s^4)$ correction to the potential for a general color representation. The $\mathcal{O}(\alpha_s^4 \log \alpha_s)$ ultra-soft correction, as well as the complete expression for the potential up to $\mathcal{O}(\alpha_s^4)$ and $\mathcal{O}(\alpha_s^4 \log \alpha_s)$, are given in Sec. 3. Sec. 4 gives an analysis of the color factors in perturbative computations up to 3 loops. We examine the effects of the Casimir scaling violation for various representations in Sec. 5. Concluding remarks are given in Sec. 6.

2 Wilson loop and 3-loop static potential

We consider the (vector) gauge theory for a general gauge group G with n_l massless fermions in the fundamental representation. In the case $G = SU(3)$, the theory is QCD with n_l flavors of massless quarks, which is our main concern. Nevertheless, to keep generality, all our formulas will be presented for the general gauge group.

We define the static potential between the color sources in a general representation R, in the singlet channel.[2] For this purpose we first define the vacuum expectation value

[2] Potentials in non-singlet channels are defined by inserting appropriate projection operators on the

	$SU(N)$	$SO(N)$
N_F	N	N
N_A	N^2-1	$N(N-1)/2$
C_F	$(N^2-1)/(2N)$	$(N-1)/4$
C_A	N	$(N-2)/2$
T_A	N	$(N-2)/2$
$d_F^{abcd}d_F^{abcd}/(N_AT_F)$	$(N^4-6N^2+18)/(48N^2)$	$(N^2-N+4)/192$
$d_F^{abcd}d_A^{abcd}/(N_AT_F)$	$N(N^2+6)/24$	$(N-2)(N^2-7N+22)/192$
$d_F^{abcd}d_A^{abcd}/(N_AT_A)$	$(N^2+6)/48$	$(N^2-7N+22)/192$
$d_A^{abcd}d_A^{abcd}/(N_AT_A)$	$N\,(N^2+36)/24$	$(N^3-15N^2+138N-296)/192$

Table 1: Some of the color factors related to the fundamental (vector) and adjoint representations ($R=F$ and $R=A$, respectively) in the case $G=SU(N)$ and $G=SO(N)$. Our convention is $T_F=1/2$.

of the Wilson loop as

$$W_R[C] = \langle 0|\,\hat{\mathcal{T}}\Big[\mathrm{Tr}\,\mathrm{P}\exp\Big\{ig_s\oint_C dz^\mu A_\mu^a(z)T_R^a\Big\}\Big]|0\rangle/\langle 0|\mathrm{Tr}\,\mathbf{1}_R|0\rangle\,. \tag{1}$$

Here, $\hat{\mathcal{T}}$ denotes the time-ordering of the gauge field operators $A_\mu^a(z)$. The hermitian generators of a general representation R are denoted by T_R^a, which satisfy the commutation relation $[T_R^a,T_R^b]=if^{abc}T_R^c$ with the structure constant f^{abc} of the gauge group G. The fundamental and adjoint representations, respectively, will be denoted explicitly by $R=F$ and $R=A$. The trace Tr is taken in the representation R, and $\mathbf{1}_R$ denotes the identity. P stands for the path-ordering of T_R^a along the contour C, which is a rectangular loop of spatial extent r and time extent T; see Fig. 1.

The normalization of T_R^a is given by

$$\mathrm{Tr}(T_R^aT_R^b) = T_R\,\delta^{ab}. \tag{2}$$

We fix our convention by setting $T_F=1/2$. The dimension of the representation R is denoted by N_R. The quadratic Casimir operator as well as symmetric invariant tensors which will appear in our computation are defined as

$$(T_R^aT_R^a)_{ij} = C_R\delta_{ij}, \tag{3}$$

$$d_R^{a_1\ldots a_n} = \frac{1}{n!}\sum_\pi \mathrm{Tr}\left(T_R^{a_{\pi(1)}}\ldots T_R^{a_{\pi(n)}}\right), \tag{4}$$

where the sum is over all permutations π of the indices. There are a number of relations satisfied by these color factors; see [18]. We note two of them: (i) $T_RN_A=C_RN_R$, which

Wilson loop at temporal boundaries. Presently the potential for the fundamental representation in the octet channel is known up to 2-loop order [17].

follows from eq. (3) after taking trace; (ii) $d_A^{a_1\cdots a_n} = 0$ for odd n's, since $(T_A^a)^T = -T_A^a$. Some values of the color factors are listed in Tab. 1 for $G = SU(N)$ and $G = SO(N)$.

The static potential between the color sources in a general representation R is defined from the Wilson-loop expectation value as

$$V_R(r) = \lim_{T\to\infty} \frac{1}{(-iT)} \log(W_R[C])\,. \tag{5}$$

In other words, the potential appears in $W_R[C]$ in an exponentiated form for large T, $W_R[C] \sim \exp\{-iTV_R(r)\}$.

We may evaluate $V_R(r)$ using perturbation theory. Since our technology for loop computations is developed mostly in momentum space, we compute the potential in momentum space. In order to regularize both UV and IR divergences, we employ dimensional regularization with one temporal dimension and $d = D - 1 = 3 - 2\epsilon$ spatial dimensions. Thus, the perturbative potential expressed in terms of the corresponding (V-scheme) coupling in momentum space reads

$$V_R^{\rm PT}(r) = \left(\frac{\mu^2 e^{\gamma_E}}{4\pi}\right)^{\epsilon} \int \frac{d^d\vec{q}}{(2\pi)^d}\, e^{i\vec{q}\cdot\vec{r}} \left[-4\pi C_R \frac{\alpha_{V_R}^{\rm PT}(q)}{q^2}\right], \tag{6}$$

where both quantities are denoted with superscripts PT to make explicit that they are computed in perturbative expansions of the strong coupling constant. A prefactor is included on the right-hand side such that $\alpha_{V_R}^{\rm PT}(q)$ is defined to be dimensionless; $q = |\vec{q}|$; $\gamma_E = 0.5772...$ denotes the Euler constant.

The perturbative expansion of $\alpha_{V_R}^{\rm PT}(q)$ is expressed as

$$\alpha_{V_R}^{\rm PT}(q) = \alpha_s(\mu) \sum_{n=0}^{\infty} P_n(L) \left(\frac{\alpha_s(\mu)}{4\pi}\right)^n \tag{7}$$

with

$$L = \log\left(\frac{\mu^2}{q^2}\right). \tag{8}$$

Here, $\alpha_s(\mu)$ denotes the strong coupling constant renormalized at the renormalization scale μ, defined in the modified minimal subtraction ($\overline{\rm MS}$) scheme; $P_n(L)$ denotes an nth-degree polynomial of L. The renormalization-group equation of $\alpha_s(\mu)$ is given by

$$\frac{d}{d\log(\mu^2)} \left(\frac{\alpha_s(\mu)}{4\pi}\right) = -\sum_{n=-1}^{\infty} \beta_n \left(\frac{\alpha_s(\mu)}{4\pi}\right)^{n+2}, \tag{9}$$

where β_n represents the $(n+1)$-loop coefficient of the beta function. The relevant coefficients read [19]

$$\begin{aligned}
&\beta_{-1} = \epsilon\,, \quad \beta_0 = \frac{11}{3} C_A - \frac{4}{3} n_l T_F\,, \quad \beta_1 = \frac{34}{3} C_A^2 - \left(\frac{20}{3} C_A + 4 C_F\right) n_l T_F\,, \\
&\beta_2 = \frac{2857}{54} C_A^3 - \left(\frac{1415}{27} C_A^2 + \frac{205}{9} C_A C_F - 2 C_F^2\right) n_l T_F \\
&\qquad + \left(\frac{158}{27} C_A + \frac{44}{9} C_F\right) n_l^2 T_F^2\,.
\end{aligned} \tag{10}$$

Both $V_R^{\rm PT}(r)$ and $\alpha_{V_R}^{\rm PT}(q)$ are independent of the scale μ, hence their dependences on $\log\mu^2$ are dictated by the renormalization-group equation. For $n \leq 2$, the only part of the polynomial $P_n(L)$ that is not determined by the renormalization-group equation is $a_n \equiv P_n(0)$. For $n \geq 3$, $P_n(L)$ includes IR divergences in terms of poles of ϵ and assoicated logarithms, whose coefficients are not determined by β_i's. Up to 3–loop order, they are given by

$$P_0 = a_0, \quad P_1 = a_1 + a_0\beta_0 L, \quad P_2 = a_2 + (2a_1\beta_0 + a_0\beta_1)L + a_0{\beta_0}^2 L^2,$$
$$P_3 = a_3 + (3a_2\beta_0 + 2a_1\beta_1 + a_0\beta_2)L + \left(3a_1{\beta_0}^2 + \frac{5}{2}a_0\beta_0\beta_1\right)L^2 + a_0{\beta_0}^3 L^3\,, \quad (11)$$

and

$$a_3 = \bar{a}_3 + \frac{8}{3}\pi^2 C_A^3\left(\frac{1}{\epsilon} + 3\,L\right). \quad (12)$$

The $1/\epsilon$ term represents the IR divergence [20, 21, 22], which is separated together with the corresponding scale dependence.

The first three a_n's are independent of the representation R [16]:

$$a_0 = 1\,, \quad a_1 = \frac{31}{9}\,C_A - \frac{20}{9}\,T_F\,n_l\,,$$
$$a_2 = \left(\frac{4343}{162} + 4\pi^2 - \frac{\pi^2}{4} + \frac{22}{3}\zeta_3\right)\,C_A^2 - \left(\frac{1798}{81} + \frac{56}{3}\zeta_3\right)\,C_A T_F n_l$$
$$- \left(\frac{55}{3} - 16\zeta_3\right)\,C_F T_F n_l + \left(\frac{20}{9}T_F n_l\right)^2\,, \quad (13)$$

where $\zeta_3 = \zeta(3) = 1.2020...$ denotes the Riemann zeta function $\zeta(z) = \sum_{n=1}^{\infty} 1/n^z$ evaluated at $z = 3$. Since C_R is factored out in eq. (6), and since β_n's are independent of the representation R, if all a_n's are also independent of R, the potential $V_R^{\rm PT}(r)$ satisfies the Casimir scaling.

The 3-loop non-logarithmic constant $\bar{a}_3$ for the fundamental color sources has been computed recently: the contributions with internal fermion loops in [23] and the purely gluonic contributions in [12, 13]. We repeat these calculations for the general color sources. We find

$$\bar{a}_3 = -\left(\frac{20}{9}n_l T_F\right)^3 + \left[C_A\left(\frac{12541}{243} + \frac{64\pi^4}{135} + \frac{368}{3}\zeta_3\right) + C_F\left(\frac{14002}{81} - \frac{416}{3}\zeta_3\right)\right](n_l T_F)^2$$
$$+ \left[2\,c_1\,C_A^2 + \left(-\frac{71281}{162} + 264\zeta_3 + 80\zeta_5\right)C_A\,C_F + \left(\frac{286}{9} + \frac{296}{3}\zeta_3 - 160\zeta_5\right)C_F^2\right]n_l\,T_F$$
$$+ \frac{1}{2}\,c_2\,n_l\left(\frac{d_F^{abcd}d_R^{abcd}}{N_A\,T_R}\right) + \left[c_3\,C_A^3 + \frac{1}{2}\,c_4\left(\frac{d_A^{abcd}d_R^{abcd}}{N_A\,T_R}\right)\right], \quad (14)$$

where $\zeta_5 = \zeta(5) = 1.0369....$ In the above equation, the coefficients c_i's are known only numerically:

$$c_1 = -354.859, \quad c_2 = -56.83(1), \quad [23] \quad (15)$$

and[3]

$$c_3 = 502.22(12)\,, \quad c_4 = -136.8(14) \;\; [12]\,. \tag{16}$$

We find that $\bar{a}_3$ is dependent on the representation R through the color factors $d_F^{abcd} d_R^{abcd}/(N_A T_R)$ and $d_A^{abcd} d_R^{abcd}/(N_A T_R)$. These are the leading effects of the Casimir scaling violation in perturbation theory.

One may want to include massless fermions in representations other than the fundamental representation. One may easily identify the contributions from fermions in a general representation R' by simple replacements $T_F \to T_{R'}$, $C_F \to C_{R'}$ and $d_F^{abcd} \to d_{R'}^{abcd}$ in the coefficients of n_l in the equations presented in this section.

3 Ultra-soft correction

The IR divergence contained in a_3 is an artifact of the strict perturbative expansion of the static potential $V_R(r)$ in α_s. The divergence originates from the degeneracy of the singlet and adjoint intermediate states in $W_R[C]$ within the naive perturbation theory [20]. Beyond (naive) perturbation theory, this degeneracy is known to be lifted and the IR divergence is absent. The difference between the static potential $V_R(r)$ and its perturbative expansion $V_R^{\rm PT}(r)$ can be treated systematically within the effective field theory Potential Non-relativistic QCD (pNRQCD)[4] [24], which treats ultra-soft (US) gluons and heavy quark-antiquark bound-states as dynamical degrees of freedom. This difference $V_R(r) - V_R^{\rm PT}(r)$ is given by contributions of ultra-soft degrees of freedom.

We repeat the computation of the ultra-soft contributions given in [21, 25] for the case of $V_R(r)$, taking into account the following points: (1) We change the representation of the static charge of the Wilson loop from the fundamental to the general representation R. (2) The perturbative matching between the full theory and pNRQCD is properly taken into account, such that the non-logarithmic term of $V_R(r) - V_R^{\rm PT}(r)$ is predicted correctly at $\mathcal{O}(\alpha_s^4)$. Thus, we have

$$\begin{aligned}
\delta V_R^{\rm US}(r) &\equiv V_R(r) - V_R^{\rm PT}(r) \\
&= -ig_s^2 \frac{T_R}{N_R} \int_0^\infty dt\, e^{-it\,(V_{\rm ad} - V_s)} \\
&\quad \times \langle 0|\, \hat{\mathcal{T}} \Big[\mathbf{r}\cdot\mathbf{E}^a(t) \left(\mathrm{P}\, e^{ig_s \int_0^t dt'\, A_0^c(t') T_A^c} \right)_{ab} \mathbf{r}\cdot\mathbf{E}^b(0) \Big] |0\rangle + \mathcal{O}(r^3)\,.
\end{aligned} \tag{17}$$

The term shown explicitly is the leading-order $[\mathcal{O}(r^2)]$ term in the multipole expansion in $\mathbf{r}$, where $r = |\mathbf{r}|$. All fields in the matrix element are evaluated at the spatial origin. $(T_A^c)_{ab} = -if^{abc}$ denotes the generator of the adjoint representation. V_s and $V_{\rm ad}$ denote

[3] The results of Ref. [13] are $c_3 = 502.24(1)$, $c_4 = -136.39(12)$.

[4] Strictly speaking, the name of the effective theory, as well as terminology such as "quarks" and "gluons", are adequate only in the case $G = SU(3)$. We will frequently use them for the general gauge group G, nonetheless.

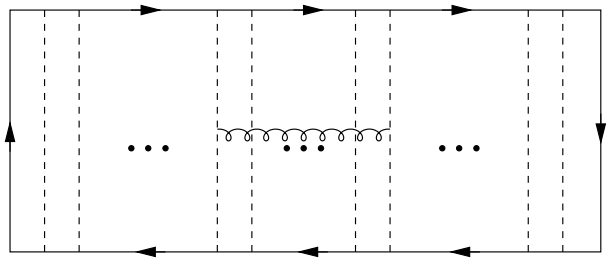

Figure 2: Class of diagrams contributing to $[\delta V_R^{\rm US}]_{\rm LO}$. Dashed lines represent Coulomb gluons, while a curly line represents transverse gluon, in Coulomb gauge.

the singlet and adjoint potentials, respectively, in the representation R, i.e., the potentials between the sources in the singlet and adjoint channels, respectively, in $R \otimes \bar{R}$.

In the distance region $r \ll \Lambda_{\rm QCD}^{-1}$, we may further expand the matrix element as well as $V_{\rm ad} - V_s$ in the coupling constant and obtain the leading–order contribution to $\delta V_R^{\rm US}(r)$ in double expansion in α_s and $\log(\alpha_s)$.[5,6] It is understood that we employ dimensional regularization, and g_s can be identified with the bare coupling constant of the full theory in the leading order. Noting that the singlet and adjoint potentials are given by

$$V_s(r) = -\frac{C_R\,\alpha_s(\mu)}{r}\,\left[\frac{(\mu^2\,r^2\,e^{\gamma_E})^\epsilon\;\Gamma(1-2\epsilon)}{\Gamma(1-\epsilon)}\right] + \mathcal{O}(\alpha_s^2)\,, \tag{18}$$

$$V_{\rm ad}(r) = -\frac{\left(C_R - \frac{1}{2}\,C_A\right)\,\alpha_s(\mu)}{r}\,\left[\frac{(\mu^2\,r^2\,e^{\gamma_E})^\epsilon\;\Gamma(1-2\epsilon)}{\Gamma(1-\epsilon)}\right] + \mathcal{O}(\alpha_s^2)\,, \tag{19}$$

we obtain

$$\begin{aligned}\left[\delta V_R^{\rm US}(r)\right]_{\rm LO} &= -g_s^2\,C_R\frac{d-1}{d}\,r^2\,\left(\frac{(V_{\rm ad}-V_s)^2}{4\pi}\right)^{d/2}\,\left[\frac{\Gamma(1+d)\Gamma(-d)}{\Gamma(\frac{d}{2})}\right] \\ &= \frac{C_R\,C_A^3\,\alpha_s(\mu)^4}{24\pi r}\,\left[\,\frac{1}{\epsilon} + 4\log\left(\mu^2 r^2\right) - 2\log\left(C_A\alpha_s(\mu)\right) + \frac{5}{3} + 6\gamma_E\,\right]\,,\end{aligned} \tag{20}$$

where we dropped $\mathcal{O}(\epsilon)$ terms in the last expression. Since $[\delta V_R^{\rm US}]_{\rm LO}$ depends on the representation R only through the overall factor C_R, Casimir scaling is preserved by this contribution. The $1/\epsilon$ term represents the UV divergence of $[\delta V_R^{\rm US}]_{\rm LO}$ within pNRQCD effective theory. Upon Fourier transform, the $1/\epsilon$ and $\log(\mu^2)$ terms of eqs. (12) and (20) cancel each other.

We made a cross check of eq. (20) as follows. It was first pointed out in [20] that $[\delta V_R^{\rm US}]_{\rm LO}$ may be obtained as the difference between the resummation of Coulomb ladder

[5] One can verify that indeed $\delta V_R^{\rm US}(r) = V_R(r) - V_R^{\rm PT}(r)$ vanishes in the strict perturbative expansion, by expanding also $e^{-it\,(V_{\rm ad}-V_s)}$ in α_s; in this case, each integral becomes scaleless, and therefore it vanishes in dimensional regularization.

[6] $\mathcal{O}(r^3)$ terms in eq. (17) do not contribute to the leading order of this double expansion.

diagrams, given in Fig. 2, and the sum of the individual diagrams (in Coulomb gauge).[7] Namely, $[\delta V_R^{\rm US}]_{\rm LO}$ may be computed more directly using a resummation of diagrams in perturbation theory, without recourse to pNRQCD effective theory. One can verify that this is indeed the case, including the non-logarithmic terms in eq. (20). Formally the equivalence of the two approaches can be shown using the threshold expansion of Feynman diagrams [26]. We have also evaluated the relevant diagrams directly and confirmed the coefficients of the logarithms as well as the non-logarithmic constant explicitly. In the resummation approach, one can avoid complexity related to the matching of the full theory to pNRQCD, in computing the non-logarithmic terms. (See also [27].)

For completeness, we present the formula for $V_R(r)$, as given by the sum of $V_R^{\rm PT}(r)$ and $\delta V_R^{\rm US}(r)$, including all the corrections up to $\mathcal{O}(\alpha_s^4)$ and $\mathcal{O}(\alpha_s^4 \log \alpha_s)$. Namely we use the series expansion (7) up to $n = 3$ for the former and eq. (20) for the latter. We obtain

$$\Big[V_R(r)\Big]_{\rm NNNLO} = -C_R \frac{\alpha_s(\mu)}{r} \sum_{n=0}^{3} \widetilde{P}_n(L') \left(\frac{\alpha_s(\mu)}{4\pi}\right)^n , \tag{21}$$

where

$$L' = \log(\mu^2 r^2) + 2\gamma_E \,, \tag{22}$$

and

$$\widetilde{P}_0 = a_0, \quad \widetilde{P}_1 = a_1 + a_0\beta_0 L', \quad \widetilde{P}_2 = a_2 + (2a_1\beta_0 + a_0\beta_1)L' + a_0{\beta_0}^2\Big(L'^2 + \frac{\pi^2}{3}\Big),$$

$$\begin{aligned}\widetilde{P}_3 = {} & \bar{a}_3 + \delta a_3^{\rm US} + (3a_2\beta_0 + 2a_1\beta_1 + a_0\beta_2)L' \\ & + \Big(3a_1{\beta_0}^2 + \frac{5}{2}a_0\beta_0\beta_1\Big)\Big(L'^2 + \frac{\pi^2}{3}\Big) + a_0{\beta_0}^3(L'^3 + \pi^2 L' + 16\zeta_3)\,,\end{aligned} \tag{23}$$

with

$$\delta a_3^{\rm US} = \frac{16}{3}\pi^2 C_A^3 \Big[\log\Big(C_A\alpha_s(\mu)\Big) + \gamma_E - \frac{5}{6}\Big]\,. \tag{24}$$

By definition $[V_R(r)]_{\rm NNNLO}$ is a renormalization-group invariant quantity and is free from IR divergences. Apart from the overall factor C_R, only $\bar{a}_3$ in the above expression is dependent on the representation R, which is the source of the violation of the Casimir scaling.

Let us comment on the non-perturbative contributions to the static potential $V_R(r)$. At $r < \Lambda_{\rm QCD}^{-1}$, the multipole expansion in r of $\delta V_R^{\rm US}(r)$, given in eq. (17), constitutes an operator-product-expansion of $\delta V_R^{\rm US}(r)$. In this way, one can systematically parametrize the non-perturbative contributions to $\delta V_R^{\rm US}(r)$ [and therefore to $V_R(r)$] in terms of matrix elements of non-local gluon condensates, after subtracting UV divergences. See [21, 9, 10, 28] for analyses of the non-perturbative contributions to $V_R(r)$ in this framework. $[\delta V_R^{\rm US}]_{\rm LO}$ can be regarded as defining a scheme for subtracting the UV divergence at leading order, or equivalently, as defining a scheme for the corresponding non-perturbative contributions.

[7] To be precise, one should replace $C_A/2 - C_R$ by $C_A/2$ in the latter (individual) diagrams, in order to take into account the shift of the ground-state energy $0 \to V_s(r)$ by Coulomb resummation.

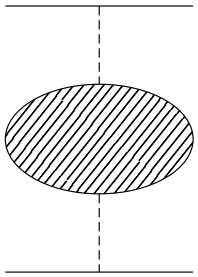

Figure 3: Class of diagrams contributing to the potential at 1-loop in Coulomb gauge. The hatched part represents the vacuum polarization of the Coulomb gluon.

4 Color factors in loop diagrams

We examine the general structure, especially the R dependence, of the color factors in $V_R^{\rm PT}(r)$ without going into details of the loop integrals. A discussion on this subject up to 2 loops is given briefly in [16]. We extend the argument to 3 loops and to more details.

At tree-level, the color factor of the potential is simply $\mathrm{Tr}(T_R^a T_R^a)/\mathrm{Tr}(\mathbf{1}_R) = C_R$. As is well-known, a simple way to understand the color factor at 1-loop order is to consider the corrections in Coulomb gauge. In this gauge, only the vacuum polarization of the Coulomb gluon contributes to the potential [29]; see Fig. 3. Since the vacuum polarization is independent of R and is proportional to δ^{ab}, the R-dependence of the potential is the same as the tree-level potential. The same argument cannot be used for the 2-loop or higher-order corrections, however, since there are contributions from graphs other than the vacuum-polarization type. Hence, we develop a more general argument.

Let us make some preparations. First, according to eq. (4), $\mathrm{Tr}(T_R^{a_1}\cdots T_R^{a_n})$ equals $d_R^{a_1\cdots a_n}$ plus a sum of the terms which include at least one commutator $[T_R^{a_i}, T_R^{a_j}]$. If we rewrite the commutator as $if^{a_i a_j b}T_R^b$ and repeat this operation recursively, we may express the trace by $d_R^{a_1\cdots a_n}$ and lower rank tensors as

$$\mathrm{Tr}(T_R^{a_1}\cdots T_R^{a_n}) = d_R^{a_1\cdots a_n} + \sum_{k=2}^{n-1} c\cdot d_R(k)\,, \tag{25}$$

where in the second term on the right-hand side we suppressed the color indices; $d_R(k)$ represents a kth-rank invariant tensor; c is an R-independent coefficient and expressed in terms of f^{abc}. ($d_R(k)$ and c have appropriate color indices which are not shown.) Contracting both sides with $f^{a_i a_j b}$, where $\{a_i, a_j\} \subset \{a_1, \ldots, a_n\}$, the first term on the right-hand side drops. Hence, we have

$$f^{a_i a_j b}\,\mathrm{Tr}(T_R^{a_1}\cdots T_R^{a_n}) = \sum_{k=2}^{n-1}\sum c'\cdot d_R(k)\,, \tag{26}$$

where we absorbed $f^{a_i a_j b}$ in c'. Note that on the left-hand side there are n generators T_R^a, while the highest rank of the invariant tensor on the right-hand side is $n-1$.

In perturbative computations of the static potential, one first eliminates iterations of lower-order potentials from the diagrams contributing to the expectation value of the

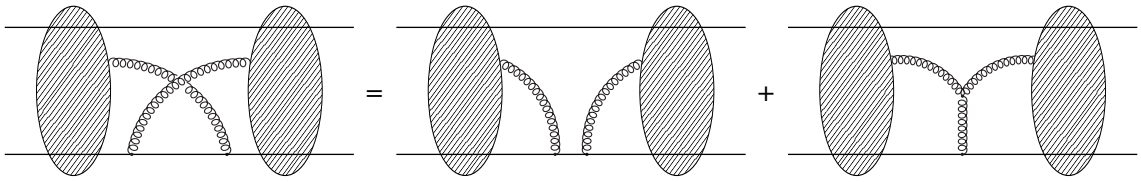

Figure 4: Reduction of a 2PI color graph to a 2PR graph and a residual graph using the identity $T_R^a T_R^b = T_R^b T_R^a + i f^{abc} T_R^c$. The 2PR graph (first graph on the right-hand side) will be deleted. In the second graph, the number of vertices on the static line is reduced by one.

Wilson loop, $W_R[C]$. A prescription has been developed, in association with a proof for the exponentiation of the static potential [30]. Let us briefly review the prescription. Within the diagrams for $W_R[C]$, only the 2-particle-irreducible (2PI) diagrams contribute to the potential. Here, 2-particle irreducibility is defined with respect to cutting the two static time-like lines simultaneously. Furthermore, among the 2PI diagrams, the color factors of the diagrams, which become 2-particle reducible (2PR) by sliding vertices on the two static lines, need to be modified; this is because, part of these diagrams are identified with iterations of lower-order potential.[8] How to modify the color factors of these diagrams is the essence of the prescription. One associates a "color graph" with each of these diagrams. Let us denote the original 2PI diagram by D and the corresponding color graph by $C_0(D)$. To begin with, the topology of the color graph $C_0(D)$ is taken to be the same as that of D, and the value of $C_0(D)$ is set equal to the color factor of the diagram D. Then one tries to render the color graph $C_0(D)$ to a 2PR graph by sliding vertices on the two static lines. Whenever any two vertices a and b on a same line are interchanged in this procedure, one separates $C_0(D)$ into two color graphs $C_1(D)$ and $C_2(D)$, corresponding to $T_R^a T_R^b = T_R^b T_R^a + [T_R^a, T_R^b]$. In the latter graph, the two vertices are combined to a single vertex on the line, corresponding to $i f^{abc} T_R^c$; see Fig. 4. Thus, the value of $C_2(D)$ equals the value of $C_0(D)$ except that $T_R^a T_R^b$ is replaced by $i f^{abc} T_R^c$. This procedure is repeated for each color graph, until no more reduction of any of the 2PI graphs into a 2PR graph is possible. Then one deletes all the 2PR graphs. The sum of the values of the remaining 2PI color graphs $\sum_{i\in 2\mathrm{PI}} C_i(D)$ is the color factor that should be assigned to the original diagram D.

After applying the above prescription, (the value of) any of the color graphs $C_i(D)$, which correspond to a general 2PI diagram D, can be written in the form

$$\begin{aligned} C_i(D) &= \mathrm{Tr}(T_R^{a_1} \cdots T_R^{a_n})\, X_n^{a_1 \ldots a_n} \\ &= N_R C_R \times \left[\frac{X_2^{aa}}{N_A} + \frac{1}{N_A T_R} (d_R^{abc} X_3^{abc} + \cdots + d_R^{a_1 \ldots a_n} X_n^{a_1 \ldots a_n}) \right], \end{aligned} \tag{27}$$

where $X_k^{a_1 \ldots a_k}$'s are independent of R. In the second equality, we substituted eq. (25)

[8] If the gauge group is abelian, any diagram, which becomes 2PR by sliding vertices on the two time-like lines, does not contribute to the potential. This is because, these diagrams (at a fixed order) sum up exactly to the exponentiation of the lower-order diagrams which contribute to the potential, if we can ignore orderings of T_R^a's.

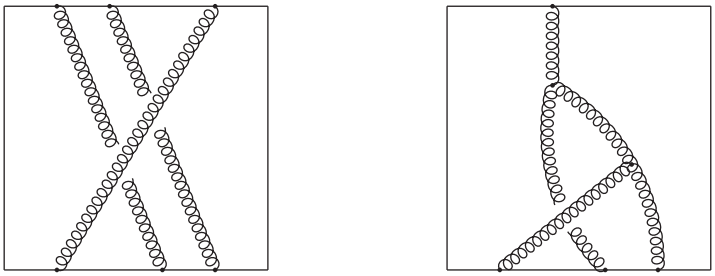

(a) (b)

Figure 5: (a) 2-loop diagram D with $n = 6$, and (b) the corresponding color graph $C(D)$ with $n_c = 4$. Starting from the diagram (a), move the right-most vertex on the upper line to the left by interchanging the vertices twice; after removing the 2PR graphs, one is left with the 2PI color graph (b).

and used $d_R^{ab} = T_R\delta^{ab}$, $T_R = N_R C_R/N_A$. The overall factor N_R will be canceled in the potential by the denominator $\mathrm{Tr}(\mathbf{1}_R) = N_R$. Each term of $X_k^{a_1\cdots a_k}$ is not factorizable (e.g. X_4^{abcd} does not include a term of the form $A^{ab}B^{cd}$), since a factorizable term corresponds to a 2PR color graph.[9] We will see this in explicit examples below.

We note that, in eq. (27), purely gluonic contributions to $X_k^{a_1\cdots a_k}$ (expressed in terms of only f^{abc}'s) for an odd k vanish, at least up to fairly high orders in perturbative computations, and it is definitely true up to 3 loops. This is because, $X_k^{a_1\cdots a_k}$ can be expressed with only invariant tensors $d_A^{b_1\cdots b_j}$'s (f^{abc}'s can be eliminated) up to certain high orders [18]. Since $d_A^{a_1\cdots a_j} = 0$ for an odd j, $d_R^{a_1\cdots a_k} X_k^{a_1\cdots a_k}$ should vanish.[10]

Now we are in a position to discuss the loop diagrams. We start from 2-loops. Let us denote by n the number of vertices on the Wilson loop in a 2PI diagram D. Then we examine, for each fixed $n(\leq 6)$, the corresponding color graphs. Consider a diagram D with $n = 6$ or $n = 5$. The diagram does not include fermion loops. The number of vertices on the Wilson loop in the corresponding color graphs $C(D)$ is $n_c = 4$; see Fig. 5. The color graphs have a form $C(D) = \mathrm{Tr}(T_R^{a_1}\cdots T_R^{a_4})\, X_4^{a_1\cdots a_4}$. Each term of $X_4^{a_1\cdots a_4}$ is expressed by two structure constants $f^{abc}f^{cde}$ with a different assignment of indices. We rewrite $\mathrm{Tr}(T_R^{a_1}\cdots T_R^{a_4})$ in terms of d_R's using eq. (25). Then $C(D)$ is expressed in the form of eq. (27). There is, however, no way of contracting indices such that d_R^{abcd} survives. Since X_3^{abc} is zero in the pure gluonic case, the only remaining term is X_2^{aa}.

We consider the diagrams D with $n = 4$. The corresponding color graphs have either of the following 3 forms: (i) $C(D) = \mathrm{Tr}(T_R^{a_1}\cdots T_R^{a_4})\, X_4^{a_1\cdots a_4}$ with each term of $X_4^{a_1\cdots a_4}$ expressed by two structure constants; (ii) $C(D) = \mathrm{Tr}(T_R^a T_R^b T_R^c)\, X_3^{abc}$; (iii) $C(D) = \mathrm{Tr}(T_R^a T_R^b)\, X_2^{ab}$. The case (i) is the same as $n = 5$,6. In the case (ii) the purely gluonic

[9] 2PR color graphs, which are deleted, contain powers of C_R if they contain (for instance) iterations of the tree graph, $X_k^{a_1\cdots a_k} \propto \delta^{a_1a_2}\delta^{a_3a_4}\cdots$, since $T_R^aT_R^a = C_R\mathbf{1}_R$.

[10] Furthermore, if we take a sum $C_i(D) + C_i(\bar{D})$, where $C_i(\bar{D}) = (-1)^n\mathrm{Tr}(T_R^{a_n}\cdots T_R^{a_1})\, X_n^{a_1\cdots a_n}$, in the sum, purely gluonic contributions to $d_R^{a_1\cdots a_k}X_k^{a_1\cdots a_k}$ for an odd k vanish to all orders. Note that, due to the charge conjugation symmetry, if there is a color graph $C_i(D)$, there is also a conjugate graph $C_i(\bar{D})$, unless the two graphs are the same.

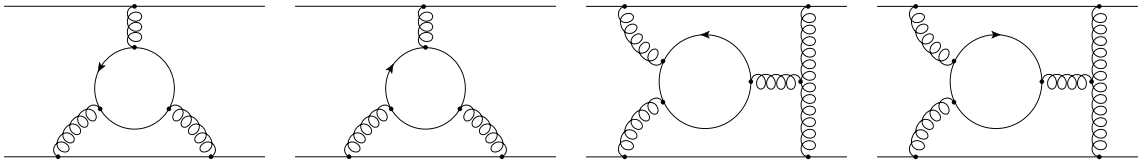

Figure 6: Pairs of color graphs with a fermion loop: (a)(b) 2-loop graphs; (c)(d) 3-loop graphs. The graphs in each pair have the same topology and the opposite charge flow directions in the fermion loops. The d_F^{abc} part of $\mathrm{Tr}(T_F^a T_F^b T_F^c)$ cancel between each pair.

contribution to the $d_R^{abc} X_3^{abc}$ term vanishes, as we already noted; on the other hand, the contributions of graphs with a fermion loop to $d_R^{abc} X_3^{abc}$ is proportional to $f^{abc} d_R^{abc} = 0$, since the fermion loop is included as a gluon vacuum polarization. The case (iii) is of the type X_2^{aa} by itself. Thus, $C(D)$ has only the X_2^{aa} term in all three cases.

The color graphs, which corresponds to the diagrams with $n = 3$, are either in the form $\mathrm{Tr}(T_R^a T_R^b T_R^c)\, X_3^{abc}$ or $\mathrm{Tr}(T_R^a T_R^b)\, X_2^{ab}$. The only new aspect, as compared to the cases (ii) and (iii) of $n = 4$, is in the diagrams including a fermion loop which has three vertices on it. These diagrams are proportional to $n_l \mathrm{Tr}(T_F^a T_F^b T_F^c) = n_l (d_F^{abc} + \frac{i}{2} T_F f^{abc})$. The $n_l d_F^{abc}$ part is canceled between a pair of color graphs with the same topology but with the opposite charge flows of the fermion loop; see Figs. 6(a)(b). This is because $\mathrm{Tr}(T_F^a T_F^b T_F^c) - \mathrm{Tr}(T_F^c T_F^b T_F^a) = i T_F f^{abc}$. Thus, the sum of such a pair of color graphs is $n_l T_F$ times the corresponding 1-loop color graph, in which the fermion loop is replaced by the gluon three-point vertex.

The contributions of the diagrams with $n = 2$ is of the type X_2^{aa}. Hence, all the contributions are reduced to X_2^{aa} of eq. (27), which is independent of R apart from the overall factor $N_R C_R$. Thus, the Casimir scaling holds.

We can discuss the 3-loop case in a similar manner. As before, we discuss the color factors of 2PI diagrams for each fixed n, the number of vertices on the Wilson loop. The maximum number is $n = 8$.

For a moment, we consider diagrams without internal fermion loops. In the cases $n = 8, 7, 6$ and 5, the number of vertices on the Wilson loop in the corresponding color graphs $C(D)$ is $n_c = 5$ or less. In the case $n_c = 5$, the color graphs have a form $C(D) = \mathrm{Tr}(T_R^{a_1} \cdots T_R^{a_5})\, X_5^{a_1 \ldots a_5}$, and each term of $X_5^{a_1 \ldots a_5}$ contains $f^{a_i a_j b}$ ($\{a_i, a_j\} \subset \{a_1, \ldots, a_n\}$). According to eq. (26), the highest rank invariant tensor in $C(D)$ is the 4th-rank tensor d_R^{abcd}. $C(D)$ includes the X_2^{aa} and X_4^{abcd} terms of eq. (27). Each term of X_4^{abcd} includes four $f^{egh} = i(T_A^e)_{gh}$ and can be expressed as[11] $\mathrm{Tr}(T_A^{a'} T_A^{b'} T_A^{c'} T_A^{d'})$ with a different assignment of (a', b', c', d') to (a, b, c, d). There are no contractions of the indices of f^{egh}'s in the form $\mathrm{Tr}(T_A^{a'} T_A^{b'}) \mathrm{Tr}(T_A^{c'} T_A^{d'}) \propto \delta^{a'b'} \delta^{c'd'}$; these correspond to 2PR color graphs and would have generated C_R^2 had they contributed. Using eq. (25) for $R = A$, $d_R^{abcd} X_4^{abcd}$ can be expressed by $d_R^{abcd} d_A^{abcd}$. Thus, $C(D)$ is expressed by $X_2^{aa} \propto C_A^3 N_A$ and $X_4^{abcd} \propto d_A^{abcd}$.

The arguments in the other cases ($n = 2, 3, 4$ and $n_c \leq 4$ for $n = 5, 6, 7, 8$) are the

[11] Many contractions are trivially zero, such as $f^{abe} d_R^{abcd} = 0$, which are not discussed explicitly.

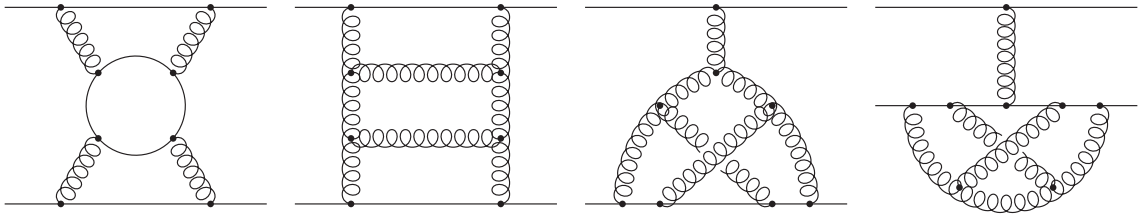

Figure 7: Some of the 2PI diagrams which contribute to $d_R^{abcd}d_F^{abcd}$ and $d_R^{abcd}d_A^{abcd}$.

same as above, apart from the point that for $n = 2, 3$ there is no X_4^{abcd} term. In the end the color factors are expressed by $X_2^{aa} \propto C_A^3 N_A$ and $X_4^{abcd} \propto d_A^{abcd}$.

Now we turn to the diagrams with fermion loops. We denote the number of vertices on a fermion loop by $n'(\leq 6)$. A fermion loop with $n' = 2$ is proportional to $n_l \mathrm{Tr}(T_F^a T_F^b) = n_l T_F \delta^{ab}$. Hence, if a 3-loop color graph includes at least one fermion loop with $n' = 2$, it is equal to $n_l T_F$ times the corresponding 2-loop graph, in which the fermion loop insertion is removed. In this case, the R dependence is only in the overall factor $N_R C_R$.

A fermion loop with $n' = 3$ is proportional to $n_l \mathrm{Tr}(T_F^a T_F^b T_F^c)$. As in the 2-loop case, the $n_l d_F^{abc}$ part is canceled between a pair of color graphs with the same topology but with the opposite charge flows of the fermion loop; see Figs. 6(c)(d). Thus, the sum of such a pair of color graphs is $n_l T_F$ times the corresponding 2-loop color graph, in which the fermion loop is replaced by the gluon three-point vertex.

A fermion loop with $n' = 4$ is proportional to $n_l \mathrm{Tr}(T_F^a T_F^b T_F^c T_F^d)$, $n_l \mathrm{Tr}(T_F^a T_F^b T_F^c T_F^b)$ or $n_l \mathrm{Tr}(T_F^a T_F^b T_F^c T_F^c)$, and a 3-loop color graph includes one such loop at most. The latter two traces are proportional to $n_l T_F \delta^{ab}$ and represent gluon vacuum polarizations; namely the color factors in these cases are proportional to those of lower-loop graphs. The first trace generates $n_l d_F^{abcd} d_R^{abcd}$ and lower rank tensors via eq. (25). Also in this case, the terms with $n_l d_F^{abc}$ are canceled between a pair of color graphs with the same topology but with the opposite charge flows of the fermion loop. This can be seen as follows. Due to the hermiticity of T_F^a, $\mathrm{Tr}(T_F^a T_F^b T_F^c T_F^d) + \mathrm{Tr}(T_F^d T_F^c T_F^b T_F^a) = 2\,\mathrm{Re}[\mathrm{Tr}(T_F^a T_F^b T_F^c T_F^d)]$. If we substitute eq. (25), the terms with odd numbers of f^{egh} are pure imaginary and vanish, hence only the even rank tensors d_F^{abcd} and $d_F^{ab} = T_F \delta^{ab}$ remain.

A fermion loop with $n' = 5$ is proportional to $\mathrm{Tr}(T_F^{a_1} \cdots T_F^{a_5})$ and included in diagrams with $n = 2$ and 3. In most of the corresponding color graphs, at least one pair from the indices $(a_1, \ldots, a_5)$ is contracted between the pair; in this case, the trace can be reduced to $\mathrm{Tr}(T_F^a T_F^b T_F^c)$, and the $n_l d_F^{abc}$ part is canceled between a pair of color graphs with the opposite charge flows of the fermion loop, as before. The only other type of contraction is in the form $\mathrm{Tr}(T_F^a T_F^b T_F^c T_F^d T_F^e) d_R^{ab} f^{cde}$, which can be reduced to d_R^{aa}, i.e. the X_2^{aa} term.

A fermion loop with $n' = 6$ is contained only as a gluon vacuum polarization in the diagrams with $n = 2$. Hence, they contribute only to the X_2^{aa} term of eq. (27).

In summary, up to 3-loops the Casimir scaling violating terms arise only as $d_A^{abcd} d_R^{abcd}$ and $n_l d_F^{abcd} d_R^{abcd}$ in the X_4^{abcd} term of eq. (27). Typical 2PI diagrams which contribute to these color factors are shown in Fig. 7. All the other color factors are collected in the X_2^{aa} term. The absence of the odd-rank symmetric invariant tensors d_F, d_A follows

from $(T_A^a)^T = -T_A^a$ and the cancellation between diagrams with opposite charge flows in a fermion loop. These features are ensured by the charge conjugation symmetry. Thus, the charge conjugation symmetry plays an important role in suppressing the Casimir scaling violating effects.

5 Numerical analysis of Casimir scaling violation

In this section, we examine the perturbative predictions for the Casimir scaling violation numerically and compare them with lattice computations, in the case of QCD with zero flavor of quarks (quenched approximation). For the lattice results, we will use those given in [2], as they seem to be most accurate and extensive up to date. Throughout the analysis, we use the central value of $r_0 \Lambda_{\overline{\rm MS}}^{\text{3-loop}} = 0.574 \pm 0.042$ [10] to fix the relation between the lattice scale and $\Lambda_{\overline{\rm MS}}^{\text{3-loop}}$, where r_0 denotes the Sommer scale [31]. (It is customary to interpret $r_0 \approx 0.5$ fm when comparing this scale to one of the real world.) When making comparisons, one should note the following point. As is well known, the constant (r-independent) part of the potentials by perturbative and lattice computations cannot be related unambiguously. This is because, the self-energy contribution and the potential energy contribution in a lattice computation of the Wilson loop cannot be separated unambiguously. Furthermore, it is formidable in perturbation theory to reproduce exactly the subtraction scheme used in [2], which subtracts the leading-order self-energy contribution defined in lattice perturbation theory. Alternatively, we study quantities which are, by construction, independent of the constant part of the potentials, and discuss their relation to the Casimir-scaling violating effects measured in the lattice simulation.

In this analysis we define the following two quantities as measures for violation of the Casimir scaling of the static potential for the general representation R:

$$\delta_{\rm CS}^{V_R} = \frac{[V_R(r) - V_R(r_1)]/C_R}{[V_F(r) - V_F(r_1)]/C_F} - 1\,, \tag{28}$$

$$\delta_{\rm CS}^{F_R} = \frac{V_R'(r)/C_R}{V_F'(r)/C_F} - 1\,. \tag{29}$$

Both quantities are zero if the potential has an exact Casimir scaling property. Both quantities are independent of the constant part of the potential: In the first quantity $\delta_{\rm CS}^{V_R}$, we subtracted a constant from the potential $V_R(r)$ such that it vanishes at $r = r_1$; in the second quantity $\delta_{\rm CS}^{F_R}$, we used the force $F_R(r) = -V_R'(r)$ between the color sources. The fundamental representation ($R = F$) is used as a reference in both quantities.

In principle $\delta_{\rm CS}^{V_R}$ and $\delta_{\rm CS}^{F_R}$ can be measured in lattice simulations. On the other hand, they can be computed in perturbation theory, by replacing $V_{R,F}(r)$ by $[V_{R,F}(r)]_{\rm NNNLO}$. They are equal at the leading order:

$$\delta_{\rm CS}^{V_R}, \delta_{\rm CS}^{F_R} = \left(\frac{\alpha_s(\mu)}{4\pi}\right)^3 \left[\, \frac{c_2 n_l}{2N_A} \left(\frac{d_F^{abcd} d_R^{abcd}}{T_R} - \frac{d_F^{abcd} d_F^{abcd}}{T_F} \right)\right.$$

$$+\frac{c_4}{2N_A}\left(\frac{d_A^{abcd}d_R^{abcd}}{T_R}-\frac{d_A^{abcd}d_F^{abcd}}{T_F}\right)\Bigg]+\mathcal{O}(\alpha_s^4)\,. \tag{30}$$

At this order, $\delta_{\rm CS}^{V_R}$ and $\delta_{\rm CS}^{F_R}$ are independent of r; $\delta_{\rm CS}^{V_R}$ is also independent of r_1.

Eq. (30) shows that $\delta_{\rm CS}^{V_R}$ and $\delta_{\rm CS}^{F_R}$ are negative and their absolute magnitudes increase with the color factor $n_l\, d_F^{abcd}d_R^{abcd}/(N_AT_R)$ or with $d_A^{abcd}d_R^{abcd}/(N_AT_R)$. (Note that $c_2, c_4 < 0$.) As a result, the effect of Casimir scaling violation is to reduce the tangent of $V_R(r)/C_R$ for larger $n_l\, d_F^{abcd}d_R^{abcd}/(N_AT_R)$ or for larger $d_A^{abcd}d_R^{abcd}/(N_AT_R)$. This can be seen from the fact that $\delta_{\rm CS}^{F_R}$, defined from the static force, is reduced by this effect.

As shown in [12], in the case $G = SU(3)$, $R = F$ and $n_l = 0$, the potential $[V_F(r)]_{\rm NNNLO}$ for the fundamental representation agrees fairly well with the lattice results in the distance range $0.1 \lesssim r/r_0 \lesssim 0.5$.[12] Hence, it would be natural to test whether the perturbative prediction is also capable of reproducing the Casimir-scaling violating effects in the same distance range. Generally the perturbative predictions for $\delta_{\rm CS}^{V_R}$ and $\delta_{\rm CS}^{F_R}$, eq. (30), are quite small, since they are 3-loop effects. At the same time, they turn out to be strongly scale-dependent, since only the leading-order terms with a high power of α_s are known. For example, for the adjoint (octet) potential of $SU(3)$ ($R = A$), we find

$$\begin{aligned}\delta_{\rm CS}^{V_A}, \delta_{\rm CS}^{F_A} &\approx \alpha_s^3\,(-0.129 - 0.0030\, n_l)\\ &\approx \begin{cases} -0.00032 & \left(n_l = 0,\ \mu = \mu_1 = \Lambda_{\overline{\rm MS}}^{\text{3-loop}}/0.035\right)\\ -0.0013 & \left(n_l = 0,\ \mu = \mu_2 = \Lambda_{\overline{\rm MS}}^{\text{3-loop}}/0.14\right)\end{cases}.\end{aligned} \tag{31}$$

Here, the scale μ_1 (μ_2) is the largest (smallest) scale,[13] with which the stability of $[V_R(r)]_{\rm NNNLO}$ has been examined in [12], where μ_1 and μ_2 differ by a factor of 4. It is a standard way to estimate uncertainties of the perturbative prediction for the potential. Since $\delta_{\rm CS}^{V_A}$ and $\delta_{\rm CS}^{F_A}$ are determined by the potential, we use this scale dependence to estimate uncertainties of these quantities. Hence, our estimates for $\delta_{\rm CS}^{V_A}$ and $\delta_{\rm CS}^{F_A}$ are between -0.03% and -0.13% for $n_l = 0$, in the distance range $0.1 \lesssim r/r_0 \lesssim 0.5$. The large uncertainties in the estimates are due to the strong scale dependence. The scale dependence is expected to be reduced if the higher-order corrections (beyond 3-loop) to $\delta_{\rm CS}^{V_A}, \delta_{\rm CS}^{F_A}$ are incorporated.

We list the color factors for various representations of $SU(3)$ in Tab. 2. Our estimates for $\delta_{\rm CS}^{V_R}$, $\delta_{\rm CS}^{F_R}$ for the corresponding representations are shown in the same table for $n_l = 0$. All the estimates are derived in the same way as in eq. (31). Note that in the case of $SU(3)$ simple relations

$$\left[\frac{d_F^{abcd}d_R^{abcd}}{N_AT_R}\right]_{SU(3)} = \frac{1}{8}\left(\left[C_R\right]_{SU(3)} - \frac{1}{2}\right), \tag{32}$$

$$\left[\frac{d_A^{abcd}d_R^{abcd}}{N_AT_R}\right]_{SU(3)} = \frac{9}{4}\left(\left[C_R\right]_{SU(3)} - \frac{1}{2}\right) \tag{33}$$

[12] It is estimated in Ref. [10] that, by renormalization-group improvement of $[V_R(r)]_{\rm NNNLO}$ (after subtraction of the renormalon), the agreement becomes better up to larger distances, $r/r_0 \lesssim 0.8$.

[13] They correspond to $\mu_1^{-1} \approx 0.06\, r_0$ and $\mu_2^{-1} \approx 0.24\, r_0$.

N_R	(p,q)	C_R	T_R	$\frac{d_F^{abcd}d_R^{abcd}}{N_A T_R}$	$\frac{d_A^{abcd}d_R^{abcd}}{N_A T_R}$	$\delta_{\rm CS}^{V_R}, \delta_{\rm CS}^{F_R}(\%)$ for $n_l = 0$
3	$(1,0)$	$4/3$	$1/2$	$5/48$	$15/8$	
8	$(1,1)$	3	3	$5/16$	$45/8$	-0.03 – -0.13
6	$(2,0)$	$10/3$	$5/2$	$17/48$	$51/8$	-0.04 – -0.16
15_a	$(2,1)$	$16/3$	10	$29/48$	$87/8$	-0.08 – -0.31
10	$(3,0)$	6	$15/2$	$11/16$	$99/8$	-0.09 – -0.37
27	$(2,2)$	8	27	$15/16$	$135/8$	-0.13 – -0.52
24	$(3,1)$	$25/3$	25	$47/48$	$141/8$	-0.13 – -0.55
15_s	$(4,0)$	$28/3$	$35/2$	$53/48$	$159/8$	-0.15 – -0.63
$\left[\frac{(k+1)(k+2)}{2}\right]_s$	$(k,0)$	$\frac{k(k+3)}{3}$	$\frac{k(k+1)(k+2)(k+3)}{48}$	$\frac{2k^2+6k-3}{48}$	$\frac{3(2k^2+6k-3)}{8}$	$(-0.0063$ – $-0.026)$ $\times(k+4)(k-1)$

Table 2: Color factors for $SU(3)$, for the representations $R = 3, 8, 6, 15_a, 10, 27, 24, 15_s, \left[\frac{(k+1)(k+2)}{2}\right]_s$, where each R is labeled by its dimension N_R. (p,q) denotes the weight factor. See Sec. 2 for the definitions of the other color factors. The last column represents the estimates (in per cent) of $\delta_{\rm CS}^{V_R}, \delta_{\rm CS}^{F_R}$ for $n_l = 0$. The last row represents the kth-rank completely symmetric representation.

hold, since $[d_F^{abcd}]_{SU(3)} = [d_A^{abcd}]_{SU(3)}/18 = (\delta^{ab}\delta^{cd} + \delta^{ac}\delta^{bd} + \delta^{ad}\delta^{bc})/24$. It follows that the contribution of the internal quark per each flavor is about 40 times smaller than that of the pure gluons, independently of R. Hence, the contributions of the internal quarks may be neglected in QCD in the first approximation. Eqs. (32) and (33) also show that the Casimir-scaling violations, $\delta_{\rm CS}^{V_R}$ and $\delta_{\rm CS}^{F_R}$, scale proportionally to C_R for $C_R \gg 1$ in QCD.

Let us compare our estimates with the lattice results. We may relate $\delta_{\rm CS}^{V_R}$ to the Casimir scaling violating effects measured in the lattice simulation. From Fig. 4 and the numbers listed in Tables II and IX of [2], $R_D(r)$ defined in eq. (31) of that paper is estimated to be close to $(C_R/C_F)(1 + \delta_{\rm CS}^{V_R})$ with a choice $r_1 \sim 0.05\, r_0$. Or equivalently,

$$\delta_{\rm CS}^{V_R} \approx \frac{C_F}{C_R} R_D - 1. \tag{34}$$

Since our prediction for $\delta_{\rm CS}^{V_R}$ is independent of r_1 at leading order, we can compare our predictions with the lattice results without a precise knowledge of r_1. Ref. [2] observed no violations of the Casimir scaling in R_D at $0.3 \lesssim r/r_0 \lesssim 2$ within 5% accuracy, for the representations $R = 8, 6, 15_a, 10, 27, 24, 15_s$. This translates to bounds $|\delta_{\rm CS}^{V_R}| < 5\%$ for all of these representations in the same distance range. As seen in Tab. 2, these bounds are perfectly consistent with our predictions in the overlapping distance range $0.3 \lesssim r/r_0 \lesssim 0.5$: our estimates are an order of magnitude smaller in the largest cases.

It is desirable to test our predictions in lattice simulations. On the one hand, our current estimates for $\delta_{\rm CS}^{V_R}$, $\delta_{\rm CS}^{F_R}$ have large uncertainties due to scale dependences, and only their orders of magnitude can be predicted. On the other hand, the prediction, that

these quantities scale proportionally to specific combinations of color factors as given in eq. (30), is expected to be more secure, especially for smaller r. As already stated, the Casimir scaling violation is enhanced for larger C_R in QCD. Hence, if a representation with an extremely large dimension is chosen, the violation may be detectable. For instance, if we use the kth-rank completely symmetric representation with $k = 30$, the estimates for $\delta_{\rm CS}^{V_R}$, $\delta_{\rm CS}^{F_R}$ amount to between -6% and -26%; see Tab. 2.

Another possible direction is to consider larger groups. As can be seen in Tab. 1, the color factor $d_A^{abcd}d_A^{abcd}/(N_AT_A)$ increases rapidly with N both for $G = SU(N)$ and $G = SO(N)$. However, the terms with the leading power in N cancel between $d_A^{abcd}d_A^{abcd}/(N_AT_A)$ and $d_A^{abcd}d_F^{abcd}/(N_AT_F)$. As a result $\delta_{\rm CS}^{V_A}$, $\delta_{\rm CS}^{F_A}$ scale only linearly on N for $SU(N)$ and quadratically for $SO(N)$. Thus, even if a relatively large N is chosen, it seems necessary to use higher rank representations in order to detect Casimir scaling violating effect.

There is a way to perform an indirect test, presumably with less efforts. Although the leading N dependence for $G = SU(N)$ or $G = SO(N)$ is canceled in $\delta_{\rm CS}^{V_A}$, $\delta_{\rm CS}^{F_A}$, this dependence is included in the fundamental potential $V_F(r)$. In principle, it is possible to test the contribution of the $d_A^{abcd}d_F^{abcd}/(N_AT_F)$ term in $V_F(r)$ by comparing lattice computations and $[V_F(r)]_{\rm NNNLO}$. In the case $G = SU(N)$, the contribution proportional to $d_A^{abcd}d_F^{abcd}/(N_AT_F)$ in $[V_F(r)]_{\rm NNNLO}$ (or in $[dV_F(r)/dr]_{\rm NNNLO}$) is estimated to be between -6% and -23% of the total amount for $N = 25$, and between -10% and -39% for $N = 30$, using the same values for $\alpha_s(\mu_1)$ and $\alpha_s(\mu_2)$ as the $SU(3)$ case. We may also use larger representations and test the $d_A^{abcd}d_R^{abcd}/(N_AT_R)$ term. Verifying the contribution of the $d_A^{abcd}d_R^{abcd}/(N_AT_R)$ term may be a first step toward testing the Casimir scaling violation.

6 Concluding remarks

In this paper, we computed, within perturbation theory, the full $\mathcal{O}(\alpha_s^4)$ and $\mathcal{O}(\alpha_s^4 \log \alpha_s)$ corrections to the potential $V_R(r)$ between the static color sources, defined from the Wilson loop in a general representation R of a general gauge group G. The strictly perturbative contributions and the ultra-soft contributions are separately presented. The full expression for the potential up to $\mathcal{O}(\alpha_s^4)$ and $\mathcal{O}(\alpha_s^4 \log \alpha_s)$ is also given.

One way to utilize our result is as follows. In the case $G = SU(3)$, the present result provides many observables (corresponding to different R's) which can be used in the matching procedure between lattice QCD and perturbative QCD. Already there exist a number of computations of the potentials for various R's by lattice simulations. Since the matching between both theories using the fundamental potential has been successful and can be used for the determination of α_s [10], it is expected that our present result may be used in the same way and may contribute to improve accuracies in the determination of α_s or in predicting other physical observables.

A prominent feature of our present result is that the violation of the Casimir scaling of the potential is predicted at $\mathcal{O}(\alpha_s^4)$. This is the first prediction, based on a first-principle calculation, of the Casimir scaling violation for the QCD potential. The effect

of the Casimir scaling violation is to reduce the tangent of $V_R(r)/C_R$ proportionally to $d_A^{abcd}d_R^{abcd}/(N_AT_R)$ and to $n_l\, d_F^{abcd}d_R^{abcd}/(N_AT_R)$. We studied the sizes of the Casimir scaling violation for various representations of the static sources for $G = SU(3)$. We find that they are fairly suppressed and fully consistent with the present bounds from lattice calculations, even if we take into account strong scale-dependences of the predictions. (Through a diagrammatic analysis, we observe that the suppression of the Casimir scaling violation is related to the charge conjugation symmetry.)

We also discussed possibilities that our predictions for the effects of the Casimir scaling violation may be tested for representations with large dimensions or in theories with larger gauge groups. If these tests are unreachable in near future, one may alternatively perform an indirect test of the contribution of the $d_A^{abcd}d_R^{abcd}/(N_AT_R)$ term, using the potentials for various representations of large gauge groups. If the perturbative prediction is excluded by lattice computations in these tests, it means that (at least) for the Casimir scaling violating effects non-perturbative contributions are dominant in the relevant distance region. Oppositely, suppose the perturbative prediction is positively confirmed, for instance, concerning the proportionality of the effects to the specific color factors. In this case, the tiny Casimir scaling violation may serve as another discriminant of models, which attempt to explain the nature of QCD in the long-distance as well as in the intermediate-distance regions.

It is expected that the violation of the Casimir scaling of the potential has some connection with the string breaking phenomenon, since the Casimir scaling property is known to be violated in this phenomenon. For this reason, it may be meaningful to focus on the Casimir scaling violating effects in the aforementioned class of models, even if they are tiny at $r \lesssim 1$ fm. In fact, the string breaking phenomenon is among the major dynamical issues of QCD between the intermediate and long-distance regions to be explained by these models. We may entertain some speculation from the perturbative computation. The diagrams which contribute to the Casimir scaling violations include those which (naively) are relevant in the string breaking phenomenon (for instance, the first diagram of Fig. 7 in the case $R = F$, and the second diagram in the case $R = A$). Moreover, the effect of the Casimir scaling violation is predicted to decrease the force between the static charges, indicating that screening of these charges is taking place. Although it is beyond the scope of perturbative QCD to treat the string breaking phenomenon, some hints may be revealed by investigating further the Casimir scaling violation in the distance region where perturbative treatment is still valid.

Acknowledgements

One of the authors (Y.S.) is grateful to A. Hoang and T. Onogi for fruitful discussion. The work of Y.S. is supported in part by Grant-in-Aid for scientific research No. 20540246 from MEXT, Japan.

References

[1] H. Markum and M. Faber, Phys. Lett. B **200**, 343 (1988); N. A. Campbell, I. H. Jorysz and C. Michael, Phys. Lett. B **167**, 91 (1986); S. Deldar, Phys. Rev. D **62**, 034509 (2000) [arXiv:hep-lat/9911008].

[2] G. S. Bali, Phys. Rev. D **62**, 114503 (2000) [arXiv:hep-lat/0006022].

[3] J. Ambjorn, P. Olesen and C. Peterson, Nucl. Phys. B **240**, 189 (1984); C. Michael, Nucl. Phys. B **259**, 58 (1985); L. Del Debbio, M. Faber, J. Greensite and S. Olejnik, Phys. Rev. D **53**, 5891 (1996) [arXiv:hep-lat/9510028].

[4] L. Liptak and S. Olejnik, Phys. Rev. D **78**, 074501 (2008) [arXiv:0807.1390 [hep-lat]].

[5] V. I. Shevchenko and Yu. A. Simonov, Phys. Rev. Lett. **85**, 1811 (2000) [arXiv:hep-ph/0001299].

[6] A. Pineda, Ph.D. Thesis; A. H. Hoang, M. C. Smith, T. Stelzer and S. Willenbrock, Phys. Rev. D **59**, 114014 (1999); [arXiv:hep-ph/9804227]. M. Beneke, Phys. Lett. B **434**, 115 (1998). [arXiv:hep-ph/9804241].

[7] Y. Sumino, Phys. Rev. D **65**, 054003 (2002); [arXiv:hep-ph/0104259]. S. Recksiegel and Y. Sumino, Phys. Rev. D **65**, 054018 (2002). [arXiv:hep-ph/0109122].

[8] S. Necco and R. Sommer, Nucl. Phys. B **622**, 328 (2002); [arXiv:hep-lat/0108008]; S. Recksiegel and Y. Sumino, Eur. Phys. J. C **31**, 187 (2003); [arXiv:hep-ph/0212389]. T. Lee, Phys. Rev. D **67**, 014020 (2003). [arXiv:hep-ph/0210032].

[9] A. Pineda, J. Phys. G **29**, 371 (2003). [arXiv:hep-ph/0208031].

[10] Y. Sumino, Phys. Rev. D **76**, 114009 (2007). [arXiv:hep-ph/0505034].

[11] Y. Sumino, Phys. Lett. B **571**, 173 (2003) [arXiv:hep-ph/0303120].

[12] C. Anzai, Y. Kiyo and Y. Sumino, Phys. Rev. Lett. **104**, 112003 (2010) [arXiv:0911.4335 [hep-ph]].

[13] A. V. Smirnov, V. A. Smirnov and M. Steinhauser, Phys. Rev. Lett. **104**, 112002 (2010) [arXiv:0911.4742 [hep-ph]].

[14] A. Pineda and J. Soto, Phys. Lett. B **495**, 323 (2000). [arXiv:hep-ph/0007197].

[15] N. Brambilla, X. Garcia i Tormo, J. Soto and A. Vairo, Phys. Lett. B **647**, 185 (2007).

[16] M. R. Kauth, J. H. Kuhn, P. Marquard and M. Steinhauser, Nucl. Phys. B **831**, 285 (2010) [arXiv:0910.2612 [hep-ph]].

[17] B. A. Kniehl, A. A. Penin, Y. Schroder, V. A. Smirnov and M. Steinhauser, Phys. Lett. B **607**, 96 (2005).

[18] T. van Ritbergen, A. N. Schellekens and J. A. M. Vermaseren, Int. J. Mod. Phys. A **14**, 41 (1999) [arXiv:hep-ph/9802376].

[19] O. V. Tarasov, A. A. Vladimirov and A. Y. Zharkov, Phys. Lett. B **93**, 429 (1980); S. A. Larin and J. A. M. Vermaseren, Phys. Lett. B **303**, 334 (1993) [arXiv:hep-ph/9302208].

[20] T. Appelquist, M. Dine and I. J. Muzinich, Phys. Lett. B **69**, 231 (1977); Phys. Rev. D **17**, 2074 (1978).

[21] N. Brambilla, A. Pineda, J. Soto and A. Vairo, Phys. Rev. D **60**, 091502 (1999). [arXiv:hep-ph/9903355].

[22] B. A. Kniehl, A. A. Penin, V. A. Smirnov and M. Steinhauser, Nucl. Phys. B **635** (2002) 357 [arXiv:hep-ph/0203166].

[23] A. V. Smirnov, V. A. Smirnov and M. Steinhauser, Phys. Lett. B **668**, 293 (2008), [arXiv:0809.1927 [hep-ph]].

[24] N. Brambilla, A. Pineda, J. Soto and A. Vairo, Rev. Mod. Phys. **77** (2005) 1423. [arXiv:hep-ph/0410047].

[25] B. A. Kniehl and A. A. Penin, Nucl. Phys. B **563**, 200 (1999). [arXiv:hep-ph/9907489].

[26] M. Beneke and V. A. Smirnov, Nucl. Phys. B **522**, 321 (1998) [arXiv:hep-ph/9711391].

[27] M. Beneke, Y. Kiyo and A. A. Penin, Phys. Lett. B **653** (2007) 53 [arXiv:0706.2733 [hep-ph]]; M. Beneke and Y. Kiyo, Phys. Lett. B **668** (2008) 143 [arXiv:0804.4004 [hep-ph]].

[28] Y. Koma, M. Koma and H. Wittig, Phys. Rev. Lett. **97**, 122003 (2006) [arXiv:hep-lat/0607009]; Y. Koma and M. Koma, Nucl. Phys. B **769**, 79 (2007) [arXiv:hep-lat/0609078].

[29] F. L. Feinberg, Phys. Rev. Lett. **39**, 316 (1977); F. L. Feinberg, Phys. Rev. D **17**, 2659 (1978).

[30] J. G. M. Gatheral, Phys. Lett. B **133**, 90 (1983); J. Frenkel and J. C. Taylor, Nucl. Phys. B **246**, 231 (1984).

[31] R. Sommer, Nucl. Phys. B **411**, 839 (1994) [arXiv:hep-lat/9310022].